On the Analysis of a Swarm-Intelligence Coordination Model for Swarm Robots

Caio D. D. Monteiro, Diego M. P. F. Silva and Carmelo J. A. Bastos Filho
Polytechnic School of Pernambuco, University of Pernambuco
{*cddm,dmpfs,carmelofilho*}*@ecomp.poli.br*

***Abstract*—In this paper, we propose three specific scenarios in order to allow one to analyze the performance of swarm-intelligence based coordination models for swarm of robots. The specific scenarios aim to assess some features presented on swarm robots: (i) contraction and expansion; (ii) self-segregation and self-aggregation; and (iii) the capacity to change abruptly the fly direction whenever it is necessary. We also propose a metric to analyze the cohesion of the swarm during a mission, named COE. We analyzed a recently proposed model based on the Particle Swarm Optimization technique designed to coordinate automatically swarms of robots in terms of Collision rate and COE. We performed simulations varying all the parameters in the three scenarios and we observed that the main problem is related to collisions when the width of the passageway is not much more higher than the UAVs collision radius.**

***Keywords*-Unmanned Aerial Vehicles; Swarm Robots; Swarm intelligence; Particle Swarm Optimization; Specific Scenarios.**

I. Introduction

The interest in Unmanned Aerial Vehicles (UAVs) has grown in the last years. UAVs have been applied to perform complex and sophisticated tasks, such as for agricultural applications in order to reduce the agrochemicals [1] or for search and surveillance operations [2].

Swarm intelligence have appeared in the 1990's inspired by swarms of simple creatures, such as ants, bees, birds, fireflies and fishes [3] [4]. In this case, an entity is too simple to solve complex problems, but the emergent behavior of the swarm can tackle such problems. Swarm intelligence algorithms have been successfully applied for the coordination of mobile robots [5] [6]. The application of the swarm intelligence concepts and algorithms to control and/or to coordinate mobile robots is often called swarm robotics [7].

One of the most used swarm intelligence algorithms is the Particle Swarm Optimization (PSO), proposed by Kennedy and Eberhart in 1995 [4]. In 2012, Pinheiro Silva and Bastos-Filho [5] proposed a coordination model for swarms of UAVs based on the PSO. In their model, the swarm robots present the following objectives: (i) allow the locomotion through an environment; (ii) avoid obstacles and collisions; (iii) patrol the entire environment; and (iv) detect and track targets. They analyzed communication issues and energy consumption [5], but some practical required features were not assessed in the proposed model.

In 2012, La and Sheng [8] investigated the contraction and expansion capability of a swarm of robots. They assessed the ability of the swarm to avoid obstacles, but other required features were not analyzed, such as (i) self-segregation and self-aggregation capabilities and (ii) the capacity to change abruptly the fly direction whenever it is necessary.

In this paper, we propose specific scenarios that allow one to analyze the following capabilities of the swarm: (i) contraction and expansion; (ii) segregation and aggregation; and (iii) abrupt changes of direction. Besides, we assessed the recently proposed PSO-based UAV coordination model [5] in these specific scenarios. We also propose a metric to analyze the cohesion of the swarm during a mission.

The remainder of the paper is organized as follows: the previous swarm based coodination model of UAVs is presented in Section II; the improvements in the model are presented in Section III; the simulation results are presented in Section IV; and some conclusions and future works are presented in Section V.

II. PSO-based coordination model for swarms of UAVs

The previous PSO-based coordination model proposed in [5] presents the following features: (i) locomotion mechanism, in which the UAVs obtain their localization within the environment, $\vec{x}_{uav}(t)$. This information can be acquired by a GPS; (ii) perception mechanism, whereupon each UAV has a perception sensor in order to detect targets; (iii) anti-collision mechanism, whereupon each UAV has an anti-collision sensor to avoid obstacles and to ensure a safety locomotion; (iv) and communication mechanism, whereupon every UAV owns a wireless communication device and acts as a routing bridge in to build a 2-connected ad hoc communication network.

The locomotion mechanism is guided by physical dynamical variables and parameters, such as horizontal acceleration ($\vec{a}$), maximum horizontal acceleration (a_{max}), horizontal speed ($\vec{v}$), and maximum horizontal speed (v). The $\vec{a}$ vector is composed by other vectors: synchronism ($\vec{a}_{syn}$); avoiding collisions ($\vec{a}_{col}$); avoiding losing communication ($\vec{a}_{com}$); cognitive ($\vec{a}_{cog}$); and social ($\vec{a}_{soc}$).

The Synchronism vector is given by:

$$\vec{a}_{syn} = \vec{a}_{col} + \vec{a}_{com}, \tag{1}$$

in which $\vec{a}_{col}$ and $\vec{a}_{com}$ are calculated by using the information provided by the collision and the communication sensors, respectively.

The Cognitive (related to the UAV) and Social (related to the UAV neighbor) vectors compose the swarm vector, which is given by:

$$\vec{a}_{swm} = \vec{a}_{cog} + \vec{a}_{soc}, \tag{2}$$

where $\vec{a}_{cog}$ and $\vec{a}_{soc}$ are calculated by the PSO algorithm at each iteration. Since the PSO algorithm needs a fitness function, we adopted the euclidean distance to the detected target as the quality metric for the PSO, which is given by:

$$fitness_{uav}(t) = |\vec{x}_{tar}(t) - \vec{x}_{uav}(t)|, \tag{3}$$

in which the information about target position, $\vec{x}_{tar}(t)$, is provided by the perception sensor.

The resultant acceleration is the sum of the Synchronism and the Swarm vectors.

Finally, the new UAV resultant velocity is calculated by:

$$\vec{v}(t+1) = \vec{v}(t) \cdot \omega + \vec{a}(t+1), \tag{4}$$

in which $\vec{v}(t+1)$ is the new speed, $\vec{v}(t)$ is the current speed and ω is the inertia factor.

III. Improvements in the model

Improvements were made in the previous model to allow one to assess the effects of specific scenarios in the coordination of multiple UAVs.

A. Initialization of positions of targets, obstacles and UAVs.

The previous model does not present any mechanisms that allow the precise initialization of the position of the targets and UAVs. The positions of the targets and the UAVs were initialized randomly by a uniform density function related to all environment area. A mechanism was developed to initialize the targets in desired pre-defined positions, *i.e.* the user can indicate explicitly the position of each target, obstacle and UAV.

B. Definition of trajectories of the targets

In order to assess the behavior of the swarm of robots in specific scenario, we included a tool to define the trajectories of the targets based on the definition of waypoints. This mechanism guides the targets, which attract the UAVs through the desired passageway.

C. Obstacles construction improvement

In the previous model, the obstacle were modeled as a circle with a position (p) and a radius (r). Then, the area of influence an specific obstacle is a circle in p with a radius r. In order to allow the definition of more complex obstacles, we implemented a new tool. In this new tool, an obstacle is composed by a set of line segments. The user provides an initial and a final position and, thereupon, the line segment is created. The equation for the line segment is given by:

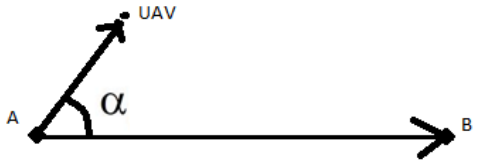

Figure 1. α angle used to determine the distance from an UAV to an obstacle.

$$Ax + By + C = 0 \ , \tag{5}$$

in which A and B are the line coefficients and C is the independent term.

When the UAV is out of the closest line segment ends, the distance between UAV and obstacle is given by Equation (6):

$$D = \sqrt[2]{(x_a - x_b)^2 + (y_a - y_b)^2}, \tag{6}$$

in which (x_a, y_a) are the coordinates of closest obstacle to the UAV and (x_b, y_b) are the coordinates of the UAV.

When the UAV is within the line segment, the distance between UAV and obstacle is given by:

$$D = \frac{|Ax_o + By_o + C|}{\sqrt[2]{A^2 + B^2}}, \tag{7}$$

in which (x_o, y_o) are the UAV coordinates, and A, B and C are the coefficients and independent term of a line segment that belongs to the obstacle.

The α angle presented in Figure 1 distinguishes the two cases aforementioned. We use Equation (6) when $cos(\alpha) < 0$, and Equation (7), otherwise.

D. Cohesion metric

A collision metric (CL) was already implemented in the previous model in order to measures the collision rate of the swarm during the mission. The collision metric is given by Equation (8):

$$CL = \frac{1}{t_{max} \cdot uav_{num}} \sum_{t=1}^{t_{max}} uav_{crt}(t), \tag{8}$$

where t_{max} is the maximum number of iterations, uav_{num} is the total number of UAVs and $uav_{crt}(t)$ is the current number of UAVs at time t.

However, a cohesion metric (COE) is also required to assess the effects of different specific scenarios in the connection degree of the swarm. Because of this, we propose here a cohesion metric, which is given by Equation (9):

$$COE = \frac{1}{t_{max} \cdot uav_{num}} \sum_{t=1}^{t_{max}} uav_{con}(t), \tag{9}$$

where t_{max} is the maximum number of iterations, uav_{num} is the total number of UAVs and $uav_{con}(t)$ is the number of

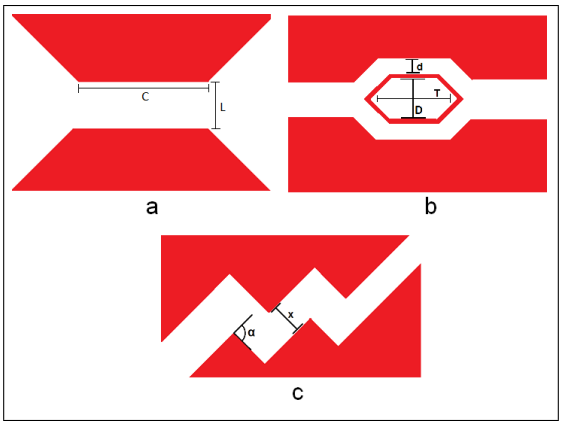

Figure 2. The three specific scenarios: (a) contraction and expansion, (b) segregation and aggregation and (c) abrupt changes of direction.

2-connected UAVs at time t. This 2-connected requirement is necessary to guarantee the functionality of the ad-hoc communication network.

IV. Simulation Results of Specific Scenarios

Three specific scenarios were developed in order to assess important features of the swarm robots coordination model. Figure 2 presents the three scenarios. The first scenario (Fig.2a) evaluates the contraction and expansion capability of the robot swarm. The second scenario (Fig.2b) assess the segregation and aggregation capability on the robot swarm. The third scenario (Fig.2c) assess the capability of the swarm to do tight turns on their movement.

A. Contraction and expansion results

The Scenario 1 (Fig.2a) is used to assess the contraction and expansion swarm capability. C and L represent the length and width of the narrowed path, respectively.

We performed analysis in this scenario varying the width and the length of the path. We used width values equal to 200 m, 400 m and 800 m, and length values equal to 20 m or 2000 m. We also assessed the coordination model performance in two different situation: maximum velocity and maximum acceleration equal to 5 m/s and 1,5 m/s^2, and 15 m/s and 4,5 m/s^2.

Table I and Table II show the mean and standard deviation values for Collisions (CL) and Cohesion (COE). Figure 3 and Figure 4 show the boxplot of CL and COE as a function of the width and length of the path, for ($5m/s$, $1,5m/s^2$) and ($15m/s$, $4,5m/s^2$), respectively.

One can observe that the coordination model did not present a good performance for widths equal 200 m and 400 m. The model presented high values for CL, specially for the narrower path. As a consequence, the cohesion of the swarm was affected. On the other hand, the length of the path does not seem to affect the performance of the model, obtaining fairly similar results for the same width. One can observe that it did not occur any single collision for width equal to 800 m.

Table I
Cohesion and Collision results for Scenario 1 with $v = 5m/s, a = 1,5m/s^2$.

	Cohesion	Collision
Length 20 m, Width 200 m		
Mean	63,20%	62,67%
Standard Deviation	7,06%	7,85%
Length 20 m, Width 400 m		
Mean	84,91%	24,67%
Standard Deviation	9,20%	5,07%
Length 20 m, Width 800 m		
Mean	99,89%	0,00%
Standard Deviation	0,00%	0,00%
Length 2000 m, Width 200 m		
Mean	49,41%	71,00%
Standard Deviation	4,85%	10,29%
Length 2000 m, Width 400 m		
Mean	79,12%	25,34%
Standard Deviation	13,75%	5,71%
Length 2000 m, Width 800 m		
Mean	99,89%	0,00%
Standard Deviation	0,00%	0,00%

Table II
Cohesion and Collision results in Scenario 1 with $v = 15m/sanda = 4,5m/s^2$.

	Cohesion	Collision
Length 20 m, Width 200 m		
Mean	63,41%	51,67%
Standard Deviation	6,94%	11,97%
Length 20 m, Width 400 m		
Mean	84,13%	20,67%
Standard Deviation	13,06%	8,68%
Length 20 m, Width 800 m		
Mean	99,66%	0,00%
Standard Deviation	0,00%	0,00%
Length 2000 m, Width 200 m		
Mean	47,35%	72,00%
Standard Deviation	2,54%	12,70%
Length 2000 m, Width 400 m		
Mean	77,70%	20,67%
Standard Deviation	15,42%	9,80%
Length 2000 m, Width 800 m		
Mean	99,67%	0,00%
Standard Deviation	0,00%	0,00%

B. Segregation and aggregation results

Scenario 2 (Fig.2b) was developed to assess the segregation and aggregation swarm capability. d is the width of the path, D is the width of the bifurcation and T is the length of the bifurcation. For this scenario, we analyzed the width and length of the bifurcation alongside with the width of the path. We used the values of 20 m and 2000 m for the width and length of the bifurcation, and 200 m, 400 m and 800 m for the width of the path.

Table III, Table IV and Table V present the results for COE and CL for the width of path equal to 200 m, 400 m

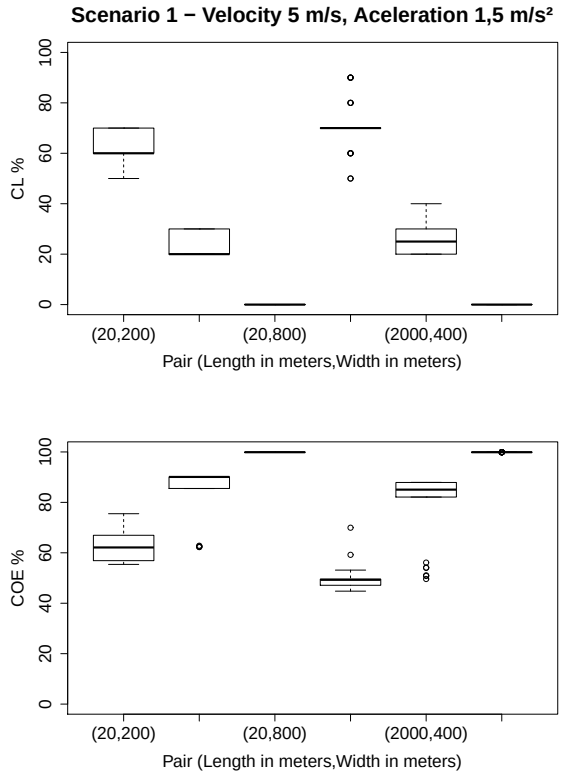

Figure 3. Analysis of CL and COE as a function of the width and length of the path, for the velocity of 5 m/s and aceleration of 1,5 m/s^2.

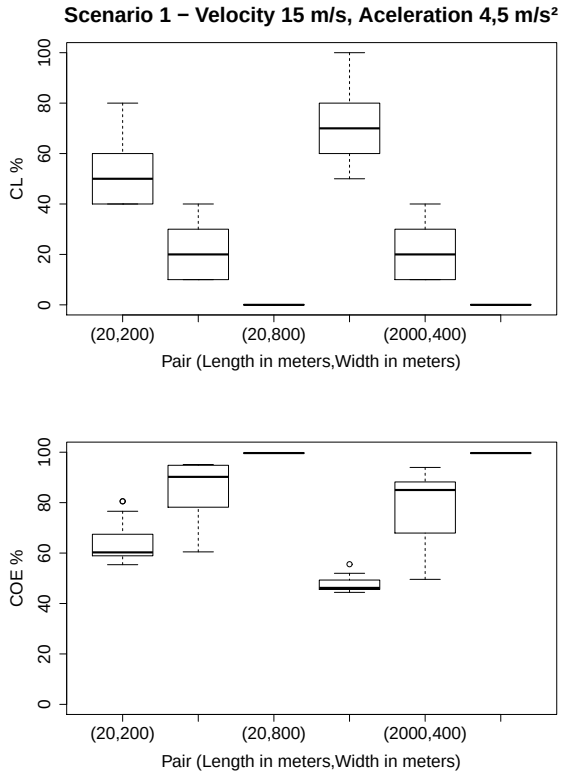

Figure 4. Analysis of CL and COE as a function of the width and length of the path, for the velocity of 15 m/s and aceleration of 4,5 m/s^2.

and 800 m, respectively. The boxplots for COE and CL are shown in Figure 5 and Figure 6, respectively.

One can observe that the swarm coordination was impaired for path width of 200 m. Besides, the presence of a bifurcation mitigates CL and COE. These effects are more evident when the bifurcation width increases. One can observe that the increase on the bifurcation width has more impact on the swarm coordination than the bifurcation length. It might occur because the obstacles are not modeled to block communication signals. This means that a bifurcation width of 200 m is not enough to break the communication among the two sub-swarms.

C. Abrupt changes of direction results

The Scenario 3 (Fig.2c) was developed to assess the swarm capability to react to tight turns presented along the trajectory. α angle is the curve inclination and x is the width of each segment of the path.

We analyzed two curve inclinations: α equal to 45° and 90°. Since we have already observed problems in narrow paths on previous scenarios, we used widths equal to 400 m, 800 m and 1600 m.

Table VI presents the results for scenario 3 and the boxplots for COE and CL are shown in Figure 7. One can observe that the results for 45° are better than the ones for

Table III
COHESION AND COLLISION RESULTS FOR SCENARIO 2 FOR WIDTH OF THE PATH 200 m.

	Cohesion	**Collision**
Length of bifurcation 200 m Width of bifurcation 200 m		
Mean	52,22%	95,00%
Standard deviation	2,20%	6,82%
Length of bifurcation 1000 m Width of bifurcation 200 m		
Mean	51,65%	90,00%
Standard deviation	1,48%	7,43%
Length of bifurcation 200 m Width of bifurcation 1000 m		
Mean	46,59%	99,67%
Standard deviation	0,59%	1,82%
Length of bifurcation 1000 m Width of bifurcation 1000 m		
Mean	48,72%	94,00%
Standard deviation	2,42%	4,99%

Table IV
COHESION AND COLLISION RESULTS FOR SCENARIO 2 FOR WIDTH OF THE PATH 400 m.

	Cohesion	**Collision**
Length of bifurcation 200 m Width of bifurcation 200 m		
Mean	63,38%	51,33%
Standard deviation	4,77%	6,81%
Length of bifurcation 1000 m Width of bifurcation 200 m		
Mean	68,59%	44,00%
Standard deviation	9,83%	11,01%
Length of bifurcation 200 m Width of bifurcation 1000 m		
Mean	56,10%	76,00%
Standard deviation	2,54%	9,68%
Length of bifurcation 1000 m Width of bifurcation 1000 m		
Mean	52,20%	81,33%
Standard deviation	1,34%	14,56%

Table V
COHESION AND COLLISION RESULTS FOR SCENARIO 2 FOR WIDTH OF THE PATH 800 m.

	Cohesion	**Collision**
Length of bifurcation 200 m Width of bifurcation 200 m		
Mean	91,24%	13,33%
Standard deviation	8,31%	6,61%
Length of bifurcation 1000 m Width of bifurcation 200 m		
Mean	89,54%	14,67%
Standard deviation	8,95%	7,30%
Length of bifurcation 200 m Width of bifurcation 1000 m		
Mean	61,88%	57,33%
Standard deviation	2,78%	10,15%
Length of bifurcation 1000 m Width of bifurcation 1000 m		
Mean	59,02%	54,67%
Standard deviation	3,33%	16,13%

α = 90°, specially for the broader paths. The effects of the curve inclination could be easily observed comparing the points $(45°, 800)$ and $(90°, 800)$ in Figure 7.

V. CONCLUSIONS

In this paper, we proposed specific scenarios in order to allow one to analyze the performance of swarm-intelligence based coordination models for swarm of robots. The specific scenarios aim to assess some features presented on swarm robots: (i) contraction and expansion; (ii) segregation and aggregation; and (iii) abrupt changes of direction. We also propose a metric to analyze the cohesion of the swarm during a mission. We analyzed a recently proposed model based on the Particle Swarm Optimization technique for UAVs coordination regarding Collision and Cohesion. We observed that the main problem is related to collisions when the width is not much more higher than the UAVs collision radius.

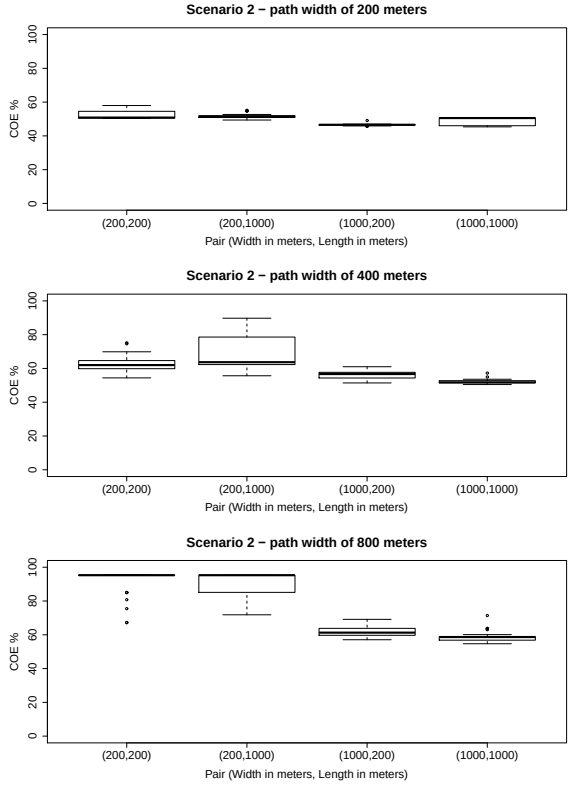

Figure 5. Analysis of COE on the scenario 2 for each configuration set.

Table VI
COHESION AND COLLISION RESULTS FOR SCENARIO 3.

	COE	**CL**
Angle 90°, Width 400 m		
Mean	17,90%	94,33%
Standard deviation	6,80%	5,04%
Angle 90°, Width 800 m		
Mean	55,31%	29,33%
Standard deviation	21,52%	9,07%
Angle 90°, Width 1600 m		
Mean	92,96%	0,34%
Standard deviation	19,56%	1,86%
Angle 45°, Width 400 m		
Mean	21,12%	71,67%
Standard deviation	12,36%	6,48%
Angle 45°, Width 800 m		
Mean	92,38%	5,33%
Standard deviation	19,94%	5,07%
Angle 45°, Width 1600 m		
Mean	92,81%	0,33%
Standard deviation	21,33%	1,83%

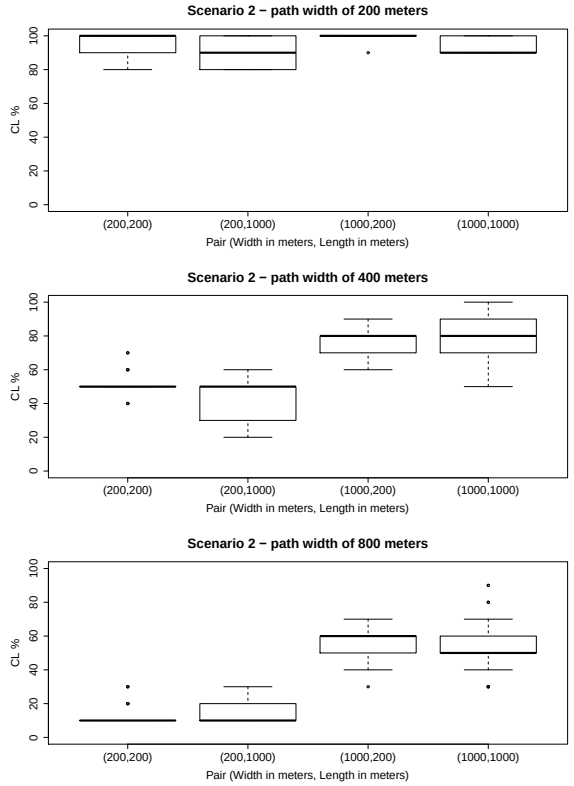

Figure 6. Analysis of CL on the scenario 2 for each configuration set.

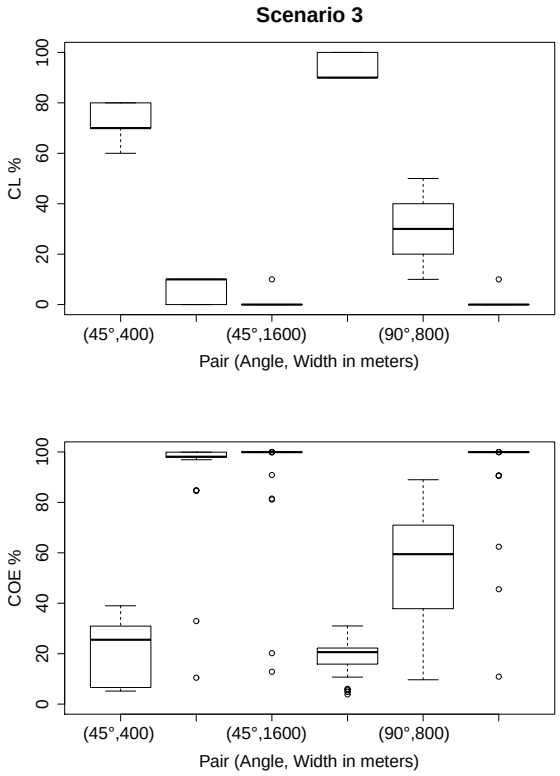

Figure 7. Analysis of COE and CL in the scenario 3.

For future work, we intend to: (i) analyze the behavior of the swarm under different types of scenarios; (ii) improve the current coordination model by including some collaborative skills in the UAVs; (iii) include mechanisms to diminish the energy consumption; (iv) add a health monitoring mechanism in order to allow UAVs to recharge in long missions; and (v) implement more realistic fluid dynamics.

REFERENCES

[1] F. G. Costa, J. Ueyama, T. Braun, G. Pessin, F. S. Osório, and P. A. Vargas, "The use of unmanned aerial vehicles and wireless sensor network in agricultural applications," in *Proceedings of IEEE International Geoscience and Remote Sensing Symposium*. Germany: IEEE, Jul. 2012.

[2] G. Varela, P. Caamamo, F. Orjales, A. Deibe, F. Lopez-Pena, and R. Duro, "Swarm intelligence based approach for real time uav team coordination in search operations," in *Nature and Biologically Inspired Computing (NaBIC), 2011 Third World Congress on*, oct. 2011, pp. 365 –370.

[3] C. J. A. Bastos-Filho, F. B. de Lima Neto, A. J. C. C. Lins, A. I. S. Nascimento, and M. P. Lima, "A novel search algorithm based on fish school behavior," in *2008 IEEE International Conference on Systems, Man, and Cybernetics*. Cingapura: IEEE, 2008.

[4] J. Kennedy and R. Eberhart, "Particle swarm optimization," in *Proceedings of IEEE International Conference on Neural Networks*, vol. 4. Perth, Austrália: IEEE, nov 1995, pp. 1942–1948.

[5] D. M. P. F. Silva, L. F. F. de Oliveira, M. G. M. Macedo, and C. J. A. B. Filho, "On the analysis of a swarm intelligence based coordination model for multiple unmanned aerial vehicles," in *Robotics Symposium and Latin American Robotics Symposium (SBR-LARS), 2012 Brazilian*, oct. 2012, pp. 208 –213.

[6] Y. Wang, A. Liang, and H. Guan, "Frontier-based multi-robot map exploration using particle swarm optimization," in *Proceedings of IEEE Symposium on Swarm Intelligence*, Apr. 2011, pp. 1–6.

[7] A. J. C. Sharkey, "The application of swarm intelligence to collective robots," in *Advances in Applied Artificial Intelligence*. John Fulcher, Idea Group Publishing, 2006, pp. 157–185.

[8] H. M. La and W. Sheng, "Dynamic target tracking and observing in a mobile sensor network," *Robotics and Autonomous Systems*, vol. 60, no. 7, pp. 996–1009, Jul. 2012.